Supersonic Jet Spectroscopy and Intramolecular Electronic Energy Transfer in Naphthalene−$(CH_2)_n$−Anthracene Bichromophoric Molecules

Xin Wang and Donald H. Levy*

Department of Chemistry and the James Frank Institute, The University of Chicago, Chicago, Illinois 60637

Mordecai B. Rubin and Shammai Speiser

Department of Chemistry, Technion − Israel Institute of Technology, Haifa 32000, Israel

Received: November 12, 1999; In Final Form: April 6, 2000

The spectroscopy and intramolecular electronic energy transfer (EET) process for a series of molecules, 9-anthryl−$(CH_2)_n$−1-naphthyl, $n = 1$, 3, and 6 (A*n*N), was investigated in a supersonic jet. For all bichromophoric molecules, the excitation spectra of the anthracene chromophore was slightly red-shifted with respect to bare anthracene and showed low-frequency vibrational progressions associated with the relative motion of the two chromophores. For A1N, when the naphthalene moiety is excited, the emission contains only anthracene-like fluorescence. From the homogeneous broadening of the absorption lines, the EET rate is estimated to be 1.5 ps. For $n = 3$ (A3N) and $n = 6$ (A6N), only the fluorescence excitation spectra of the anthracene moiety is observed. This suggests that the EET rate in A3N and A6N is much faster than that in the A1N system. Molecular geometry computations using molecular mechanics methods were applied to the interpretations of experimental results. In the case of A3N and A6N, a face-to-face conformer can be formed in which exchange coupling can be effective in enhancing the EET rate. In A1N, the bridge is sufficiently rigid that a face-to-face conformer cannot be formed.

1. Introduction

Intramolecular electronic energy transfer (Intra-EET) has been a subject of considerable interest because of its role in photophysics, photochemistry, and biology.[1] In recent years, much work[2−5] has been done in supersonic jets to investigate EET in bichromophoric molecules of the form D-B-A, where D is the energy donor, A is the energy acceptor, and B is the bridge that links the two chromophores.

The first observation of short-range Intra-EET was reported by Schnepp and Levy for the naphthalene−$(CH_2)_n$−anthracene ($n = 1-3$) system.[6] Later, many other groups examined other bichromophoric systems.[1] The occurrence of Intra-EET could be readily evaluated from knowledge of the excitation and emission spectra of each moiety alone and comparison with the corresponding spectra of the bichromophoric molecules. The basic Intra-EET process can be described by

$$\text{D*-B-A} \xrightarrow{k_{EET}} \text{D-B-A*} \qquad (1)$$

where the excitation energy is transferred from an excited donor D* chromophore to a ground-state acceptor moiety A, resulting in quenching of D* fluorescence and excitation of A. The molecular spacer bridge, B, connecting the two chromophores may play a role in promoting the transfer process. In most cases, the Intra-EET rate constant, $k_{EET,}$ is attributed to two possible contributions. The first is the long-range Coulombic contribution, which was formulated by Förster in terms of a dipole−dipole interaction.[7] The second contribution to EET is the short-range exchange interaction, as formulated by Dexter.[8] The rate of dipole−dipole induced EET decreases as R^{-6}, whereas that of the exchange-induced process decreases as $\exp(-2R/L)$, R being the interchromophore distance and L the average van der Waals radius for the overlapping orbitals. Until recently, most reported studies of Intra-EET were performed in solution where solvent effects cannot be ruled out and where complete vibrational relaxation of donor and acceptor excited electronic states may precede EET.

This paper discusses Intra-EET in the 1-naphthyl−$(CH_2)_n$−9-anthryl ($n = 1$, 3 and 6) bichromophoric system. For simplicity, we refer to the system as A*n*N throughout this paper. Figure 1 displays the molecular structure of the three bichromophoric molecules; A1N ($n = 1$), A3N ($n = 3$), and A6N ($n = 6$), along with two reference compounds, 1-methylnaphthalene (1MN) and 9-methyl-anthracene (9MA). In this bichromophoric system, D is naphthalene, A is anthracene, and B is the −$(CH_2)_n$− chain connecting the two chromophores.

Both anthracene and naphthalene have D_{2h} symmetry. Figure 2 shows the relevant energy levels and their symmetry under D_{2h}. Our investigation was focused on EET from the S_1 state of naphthalene to the S_1 state of anthracene. If the two chromophores D and A in D−B−A keep their individual spectral identities and A has sufficient quantum yield, the experimental manifestation of intramolecular EET is A-like fluorescence when D is selectively excited.

Schnepp and Levy[6] showed that the only fluorescence observed in solution came from the anthracene moiety and had spectral characteristics of anthracene emission that indicates that the excited naphthalene moiety had transferred its excitation energy completely to the anthracene moiety. This high-efficiency EET process is partly due to the good spectral overlap between the naphthalene emission and anthracene absorption spectra. These spectra are relatively broad due to many different

* To whom correspondence should be addressed.

10.1021/jp994007i CCC: $19.00
Published on Web 06/24/2000

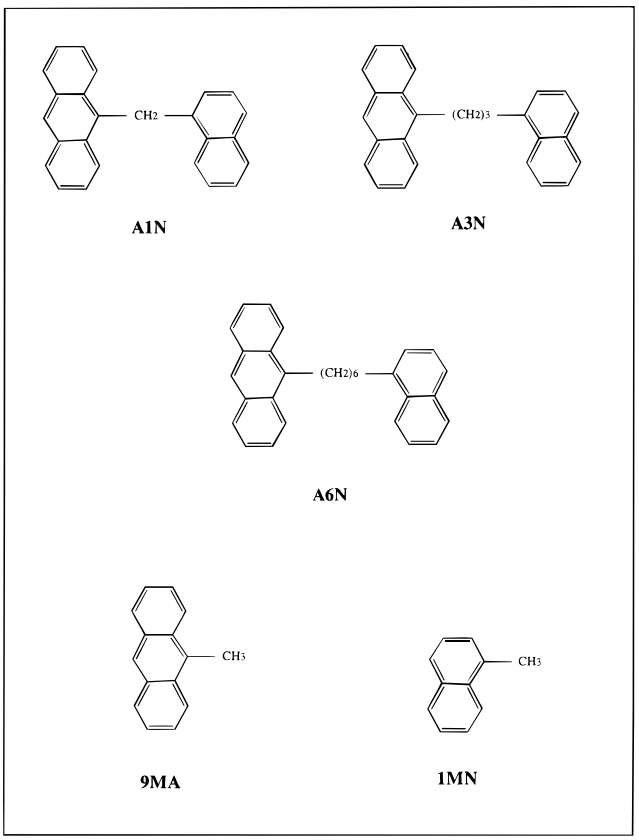

Figure 1. Structures of the molecules investigated in this paper.

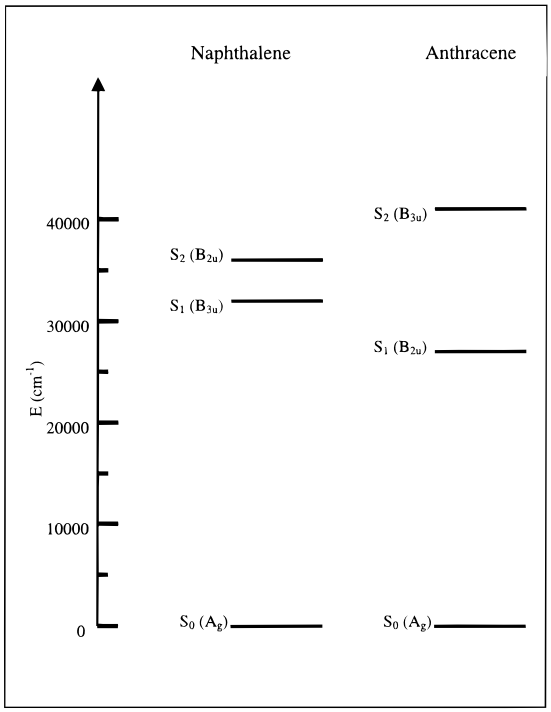

Figure 2. Singlet electronic energy levels of naphthalene and anthracene.

conformations of the floppy molecules and to solvent relaxation of the initially excited vibrational states of the molecules prior to the EET process.

The situation is expected to be different when the molecules are under supersonic jet cooling conditions. A large majority of the molecules are in their ground vibrational state and in their most stable conformation. The spectra of the molecules consist of very sharp lines, and the spectral overlap can be poor, leading to relatively slow EET and to dual fluorescence from the excited bichromophoric molecules. This is especially true for those conformations where the dipole−dipole interaction is weak and the orbital overlap is rather poor. For other conformations and spectral lines, Intra-EET may still be very efficient, as in solution at room temperature.

Although existing EET theories applicable for solution conditions can be extended to the isolated molecule case, no good estimates of the relative efficiencies of the Coulomb and exchange mechanisms are available for jet-cooled molecules.[10] If the exchange mechanism is more important, the rate should depend strongly on the overlap of the π-electronic systems of the two closely situated moieties in the molecule. If Coulomb interaction is more important, the crucial geometrical factor is the angle between the transition dipole moments of the two chromophores. Since the molecules are in their ground vibrational states belonging to their energetically most stable conformation, their geometries should strongly affect the EET rate.

Previous jet investigation of the AnN system, however, led to different results than those observed in solution.[11] From the fluorescence lifetime measurements, EET was found to be inefficient in A1N, the EET rate being comparable to the naphthalene moiety fluorescence rate. The EET rate varied with different vibronic transitions and ranged from less than 3×10^6 s^{-1} to 5×10^6 s^{-1}. For A3N, the EET rate was estimated to be 2 orders of magnitude higher than for A1N. This agreed with the solution experiment. The result for A1N, however, suggested a dramatic difference of EET efficiency between jet-cooled and room-temperature solution conditions. A similar slow EET process was observed for the naphthalene−anthracene cluster formed in a jet,[9,12] whose EET rate was estimated to be only 3.3×10^6 s^{-1}. These observations of slow EET were very unusual and unexpected. They were about 3 orders of magnitude smaller than those of other bichromophoric molecules previously studied in a jet. This naturally led to questions such as: Is the EET in A1N really so slow? Why is it so slow? If the EET process in A1N is indeed competing with the naphthalene fluorescence with a comparable rate, can fluorescence from both anthracene and naphthalene be observed when the naphthalene moiety is excited? These questions motivated us to make further investigations of the A*n*N system, particularly A1N.

2. Experimental Section

The A*n*N bichromophoric compounds were synthesized following the literature procedure[13] and were used without further purification. The melting points for A1N, A3N, and A6N were 182 °C, 92 °C, and 64 °C, respectively. During all experiments, the samples were heated in order to attain sufficient vapor pressure. The typical heating temperatures were 190 °C, 150 °C, and 200 °C, respectively. The samples were carried by helium gas at 2−3-atm stagnation pressure and expanded into the vacuum through a 100-μm pinhole.

The laser was a dye laser pumped by a Nd:YAG laser. The output of the dye laser was either frequency doubled or mixed in a KDP crystal with the fundamental frequency of the Nd:YAG laser. The resultant UV laser pulse had a duration of about 10 ns. The laser beam was directed to the vacuum chamber crossing the continuous jet, which contained the bichromophoric sample or the reference molecules.

To obtain the fluorescence excitation spectra, the total fluorescence or the filter-selected partial fluorescence was collected and recorded by a photomultiplier tube while scanning

the dye laser. Dispersed fluorescence spectra were measured using a 1.0-m monochromator and a photomultiplier tube. The details of the experimental setup can be found elsewhere.[14]

3. Results and Analysis

3.1 Anthracene and Naphthalene. Before presenting the results of the bichromophoric molecules, we briefly discuss the notation conventionally used for anthracene and naphthalene. This notation can be applied to the spectra of derivatives that contain these two chromophores and is used throughout this paper.

The bare anthracene molecule belongs to the D_{2h} point group. As illustrated in Figure 2, the S_0 state has A_g symmetry and the S_1 state has B_{2u} symmetry. The S_2 state lying about 13600 cm^{-1} above the S_1 state[15] is of B_{3u} symmetry. In the range around the S_0-S_1 transition origin, vibronic bands in the excitation and emission spectra primarily involve modes of A_g or B_{1g} symmetry. In terms of intensity, the A_g modes are dominant. In the conventional nomenclature,[16] all A_g modes are numbered according to their frequency, with "1" denoting the highest frequency mode and "12" denoting the lowest frequency mode. The numbers with bars denote the B_{1g} modes.

The bare naphthalene molecule also belongs to the point group D_{2h}. As displayed in Figure 2, the S_0 state is of A_g symmetry and the S_1 state is of B_{3u} symmetry. The S_2 state lying about 3900 cm^{-1} above the S_1 state is of B_{2u} symmetry. In the range around the S_0-S_1 transition origin, the vibronic peaks can be of either A_g symmetry or B_{1g} symmetry due to the coupling between the S_1 and S_2 states.[17] The same nomenclature[18] used for anthracene is used for naphthalene. The only difference for naphthalene is that B_{1g} modes instead of A_g modes are dominant in intensity.

The EET rate in the gas phase ranges from 10^9 s^{-1} to 10^{12} s^{-1} for molecules of the size studied here. With a laser and signal detection system having picosecond time resolution, the EET rate can be measured directly from time-domain experiments such as recording the A-like fluorescence rise time after D is excited. With nanosecond time resolution, the absolute EET rate can be derived from frequency-domain experiments in two possible ways. First, if a system has a relatively slow EET rate, fluorescence from both D and A can be observed when the D moiety is excited. In this case, the EET rate can be calculated from the relative fluorescence contribution[3] of D and A in the emission spectrum. Second, if a system has a relatively fast EET rate and only fluorescence from A is observed after exciting D, the EET rate may then be estimated from the homogeneous broadening of the D absorption peaks[11] in the fluorescence excitation spectrum. This broadening comes from the shortening of the D* lifetime as the result of EET.

3.2 Anthracene-(CH_2)-Naphthalene (A1N). *3.2.1. Fluorescence Excitation (FE) Spectra.* The total fluorescence excitation spectrum of A1N in the range of the anthracene moiety S_0-S_1 transition is shown in Figure 3a. The transition origin is at 26791 cm^{-1}, which is red-shifted 904 cm^{-1} with respect to the transition origin of bare anthracene at 27695 cm^{-1}.[15]

The vibronic bands are summarized in Table 1. The spectrum is very similar to the previously published data[11] except that some unknown peaks in the published spectrum are not seen. Those peaks might be due to impurities. Joining two free molecules via a $-CH_2-$ bridge introduces 15 extra vibrational modes in A1N (45 atoms, 129 vibrational modes) that do not exist in a combination of bare anthracene (24 atoms, 66 vibrational modes) and bare naphthalene (18 atoms, 48 vibrational modes). Some of these 15 modes are bending and torsional modes whose frequencies are tens or hundreds of reciprocal centimeters. Five of these low-frequency modes are assigned[11] and are responsible for the low-frequency vibronic bands observed in Figure 3a. The strongest peak in Figure 3a is the transition origin, and all low-frequency vibrational progressions have at the most 2 members. These facts indicate that the geometry change between the S_0 state and the S_1 state for A1N is small.

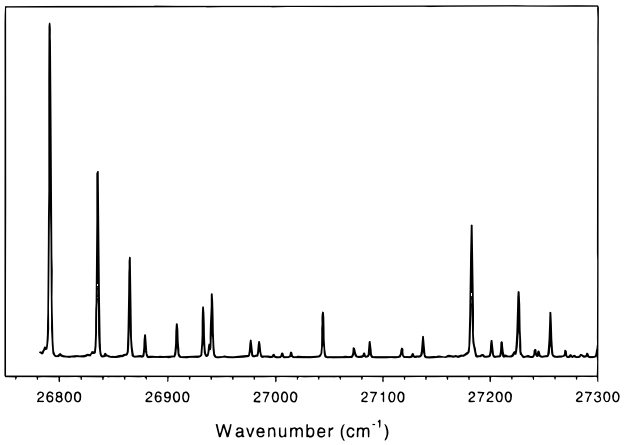

Figure 3. Total fluorescence excitation spectra of A1N in the range of the anthracene S_0-S_1 transition.

TABLE 1: Vibronic Transition Assignments for the First 550 cm^{-1} of the A1N Total Fluorescence Excitation Spectrum in the Anthracene Moiety Absorption Range

position (cm^{-1})	shift (cm^{-1})[a]	intensity[b]	assignment[c]
26 791	0	100	origin
26 835	44	56	A
26 865	74	30	B
26 879	88	7	2 × A
26 908	117	10	A + B
26 933	142	15	C
26 938	147	4	2 × B
26 941	150	19	D
26 977	186	6	A + C
26 985	194	5	A + D
27 044	253	14	E
27 073	282	3	2 × C
27 088	297	5	A + E
27 117	326	3	B + E
27 137	346	7	?
27 182	391	40	12_0^1
27 201	410	5	?
27 211	420	5	?
27 226	435	20	A + 12_0^1
27 256	465	14	B + 12_0^1
27 300	509	3	A + B + 12_0^1

[a] Blue-shifted with respect to the transition origin (26 791 cm^{-1}). [b] The transition origin is the strongest peak in the spectrum; we assign its intensity as 100. The intensities of other peaks are relative intensities compared with this peak; only peaks with relative intensities larger than 3 are listed. [c] The notation of A, B, C, D, and E is taken from ref 11.

9-Methyl-anthracene (9MA) was used as the reference to simulate the energy acceptor part of the A*n*N system. The jet spectroscopy of 9MA has been extensively studied.[19,20] The 0−0 band of 9MA is at 26933 cm^{-1}, 762 cm^{-1} red-shifted from the 0−0 band of bare anthracene.

The total fluorescence excitation spectrum of A1N in the range of the naphthalene moiety S_0-S_1 transition is shown in Figure 4a. The transition origin is at 31779 cm^{-1}. This spectrum is very similar to the published[21] spectrum of 1MN. The transition origin of the naphthalene moiety of A1N is only 6

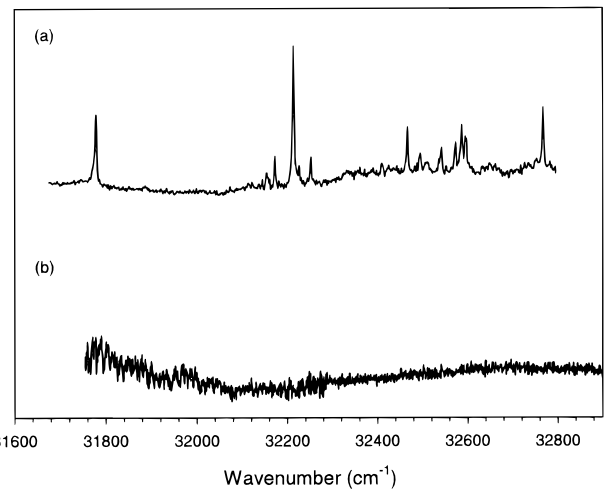

Figure 4. Total fluorescence spectra of A1N and 9MA in the range of the naphthalene S_0-S_1 transition. (a) Total fluorescence excitation spectrum of A1N in the region of the naphthalene S_0-S_1 transition. (b) Total fluorescence excitation spectrum of 9MA in the same range as (a).

TABLE 2: Vibronic Transition Assignments for the First 1000 cm^{-1} of the A1N Total Fluorescence Excitation Spectrum in the Naphthalene Moiety Absorption Range

position (cm^{-1})	shift[a] (cm^{-1})	intensity[b]	assignment
31 779	0	63	origin
32 173	394	41	?
32 214	435	100	$\bar{8}_0^1$
32 252	473	40	9_0^1
32 467	688	56	8_0^1
32 495	716	42	?
32 542	763	45	?
32 573	794	48	?
32 587	808	58	?
32 595	816	51	?
32 767	988	67	$\bar{7}_0^1$

[a] Blue-shifted with respect to the transition origin (31 779 cm^{-1}). [b] The $\bar{8}_0^1$ peak is the strongest peak in the spectrum; we assign its intensity as 100. The intensities of other peaks are relative intensities compared with this peak.

cm^{-1} blue-shifted from that of 1MN at 31773 cm^{-1}. Table 2 summarizes the assignments. All peaks still show up when a GG400 red-cut filter is put in front of the photomultiplier, indicating that the fluorescence from A1N has a component redder than 400 nm.

In Figure 4b, we show the total fluorescence excitation spectrum of 9MA in the same spectral range. In this region, approximately 5000 cm^{-1} above the S_1 state of 9MA, the spectrum of 9MA shows an absorption continuum. The absorption of A1N in this range is an overlap of sharp peaks due to the naphthalene moiety absorption and a broad continuous weak absorption background due to the anthracene moiety absorption.

3.2.2 Dispersed Fluorescence (DF) Spectra and Fluorescence Decay (FD) Spectra. For A1N, dispersed fluorescence (DF) spectra can be taken by exciting either of the two chromophores. Figure 5b shows the emission spectrum of A1N after exciting the anthracene chromophore at its 0−0 band (26791 cm^{-1}). The resolution of this spectrum is 30 cm^{-1}. This spectrum is similar to the emission spectrum obtained by exciting the transition origin of a bare anthracene molecule.[14]

Figure 5c is the emission spectrum of A1N after exciting the transition origin of its naphthalene chromophore at 31779 cm^{-1}. It was taken at a resolution of 30 cm^{-1}. The emission is anthracene-like with three broad bands appearring around

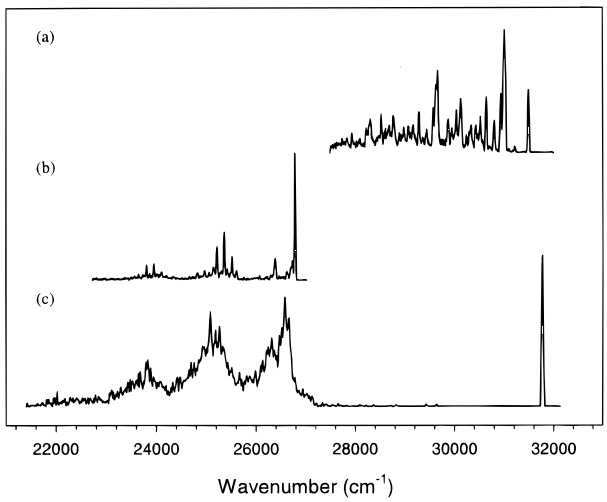

Figure 5. Dispersed fluorescence spectra of A1N and 1MN. (a) Dispersed fluorescence of 1MN excited at its transition origin (31 773 cm^{-1}). (b) Dispersed fluorescence of A1N excited at the anthracene moiety transition origin (22 6791 cm^{-1}). (c) Dispersed fluorescence of A1N excited at the naphthalene moiety transition origin (31 779 cm^{-1}). The intense feature at the exciation frequency is entirely due to scattered laser light.

TABLE 3: Assignments of Major Vibronic Peaks in the Emission Spectrum of 1MN Exciting at the Transition Origin (31773 cm^{-1})

shift (cm^{-1})[a]	intensity[b]	assignment[c]
0	51	resonance fluorescence + scattering light
486	100	$\bar{8}_1^0$
553	49	$\bar{8}_1^0 + 67$
685	27	$\bar{8}_1^0 + 199$
843	46	$\bar{8}_1^0$
960	28	$\bar{7}_1^0$
1356	44	$\bar{5}_1^0$
1442	35	$\bar{8}_1^0\bar{7}_1^0$
1608	27	$\bar{8}_1^0 7_1^0$
1824	65	$\bar{8}_1^0 5_1^0$
1907	37	$\bar{8}_1^0 5_1^0 + 67$
2195	33	$8_1^0 5_1^0$
2712	30	$2 \times 5_1^0$
2959	30	$\bar{8}_1^0 7_1^0 5_1^0$

[a] Red-shifted with respect to the excitation (31 773 cm^{-1}). [b] The $\bar{8}_1^0$ is the strongest peak in the spectrum; we assign its intensity as 100, and the intensities of other peaks are relative intensity compared with this peak. [c] Due to the low resolution, the summation of two or three modes may not exactly match the frequency of the combination modes.

23 800, 25 200, and 26 500 cm^{-1}. A fluorescence excitation spectrum of A1N was taken by passing the emitted light through a filter (GC400) that only passed light to the red of 400 nm (25 000 cm^{-1}). A spectrum taken in this way is identical to the spectrum shown in Figure 4c, where all emitted light is accepted. This indicates that all vibronic features in the naphthalene part of the A1N spectrum produce the anthracene-like emission shown in Figure 5c.

In Figure 5a, we show the emission spectrum obtained by exciting the transition origin of 1MN. It was taken with a resolution of 40 cm^{-1}. The fluorescence intensity dies off gradually beyond 27 200 cm^{-1}. The same spectrum has been reported in a previous publication,[21] but no detailed assignments were given. Our assignments for the major vibronic peaks are given in Table 3.

Figure 5c contains only anthracene-like emission, with no naphthalene-like emission at all. The strong feature at the excitation frequency is all due to scattered laser light. As seen

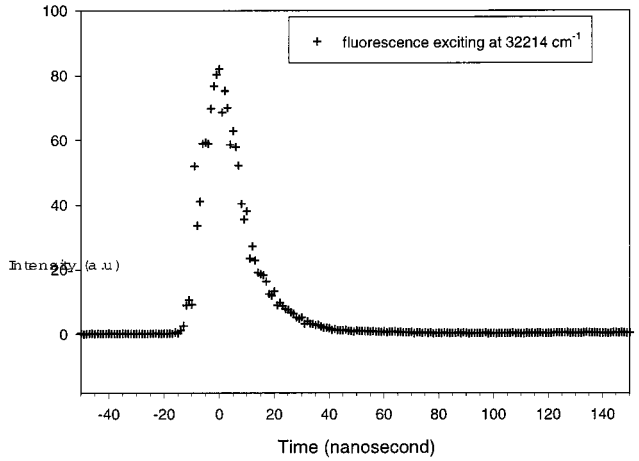

Figure 6. Fluorescence decay profile of A1N obtained by exciting the naphthalene moiety $\bar{8}_0^1$ peak (32 214 cm^{-1}).

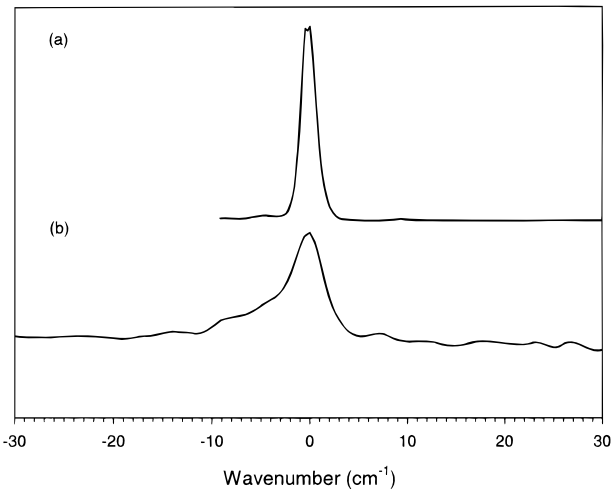

Figure 7. Profiles of the A1N fluorescence excitation peaks. (a) The transition origin of the anthracene moiety (26 791 cm^{-1}). (b) The transition origin of the naphthalene moiety (31 779 cm^{-1}).

in Figure 5a, the 1-methylnaphthalene emission spectrum contains a lot of vibronic activity. If any of the intensity at the excitation frequency were due to fluorescence rather than to scattered light, it would be accompanied by vibronic features in the region to the red of the excitation frequency. The fact that exciting the naphthalene moiety in A1N only gives anthracene-like fluorescence indicates that EET from the naphthalene chromophore to the anthracene chromophore is much faster than fluorescence from naphthalene.

The fluorescence decay obtained by exciting the $\bar{8}_0^1$ peak [32214 cm^{-1} in Figure 4a] of A1N is shown in Figure 6. The $\bar{8}_0^1$ peak was chosen instead of the transition origin because it gives the strongest signal. The emission spectrum obtained when this transition is excited is identical to that produced by excitation of the origin transition. In this figure, the fluorescence is detected without wavelength discrimination; that is, both naphthalene-like and anthracene-like fluorescence would be detected were they there. From Figure 5, we know that although it is the naphthalene moiety that is excited, all of the fluorescence in fact comes from the anthracene moiety.

From qualitative observation of Figure 6, the fluorescence lifetime is clearly less than 20 ns. We used a Gaussian function with a 10-ns fwhm as the response function to fit the fluorescence decay to a single exponential with a lifetime of 10.5 (±0.01) ns. The fluorescence lifetime of the reference compound 1MN has been measured previously.[11,22] The lifetime at the transition origin is 320 ns and decreases with excess excitation energy. States below 500 cm^{-1} excess energy all have lifetimes greater than 200 nanoseconds. The lifetime at the zero-point level of the S_1 state of naphthalene is 299 nanoseconds.[23] The lifetime of anthracene varies from 20 ns (when exciting its 0−0 transition) to 5.7 ns (when exciting its +2800 cm^{-1} transition).[24] The short lifetime observed in Figure 6 confirms what was already known from Figure 5, that energy transfer is very fast compared with the naphthalene fluorescence lifetime and that all fluorescence observed following excitation of either part of the bichromophore comes from the anthracene moiety. Were this not the case, the decay curve in Figure 6 would contain a slow component with a lifetime on the order of hundreds of nanoseconds. This measurement tells nothing about the energy transfer rate other than the fact that it is much faster than the naphthalene fluorescence rate.

3.2.3 Line Broadening. In the excitation spectrum of A1N, the lines of the naphthalene moiety are broader than the lines of the anthracene moiety. This broadening is due to the fast EET process, which shortens the naphthalene chromophore lifetime and leads to a homogeneous broadening of the spectral features.

Figure 7 compares the line width of the electronic transition origins of the naphthalene moiety and the anthracene moiety in A1N. The fwhm of the anthracene moiety (Figure 7a) is 1.86 cm^{-1}, and the fwhm of the naphthalene moiety (Figure 7b) is 4.50 cm^{-1}. Deconvoluting heterogeneous contributions to the line width[25] gives a homogeneous width of 3.95 cm^{-1} and an EET lifetime of $\tau = 1.5$ ps. This is about 5 orders of magnitude shorter than the fluorescence lifetime of the naphthalene moiety.

3.3 Anthracene−$(CH_2)_3$−Naphthalene (A3N). The 0−0 transition of A3N in the anthracene moiety S_0-S_1 region is at 26 697 cm^{-1} which is red-shifted 998 cm^{-1}, from the origin of anthracene, 236 cm^{-1} from the origin of the 9MA, and 94 cm^{-1} from the origin of A1N.[11] In the region of 0−100 cm^{-1} excess energy, there are several peaks with excess energy of 10 cm^{-1}, 22 cm^{-1}, 40 cm^{-1}, and 62 cm^{-1} (22 + 40). These peaks can be assigned as either the torsional modes of the $-(CH_2)_3-$ chain or large amplitude inter-chromophore movements. The fact that the 0−0 transition is the strongest peak in the spectrum suggests that the geometry change between S_0 and S_1 of A3N is small. The dispersed fluorescence spectrum of A3N looks much like the emission spectra of anthracene[18] and the reference compound 9MA.[19]

The total fluorescence excitation spectrum of A3N was measured in the region from 31 380 to 32 030 cm^{-1}, which is the naphthalene moiety range. The spectrum is not shown here because it contains only an absorption continuum due to the anthracene moiety. In contrast to the result of A1N (Figure 4a) and the previously published data for A3N,[11] our spectrum for A3N in this range does not contain any sharp peaks.

It is interesting that no sharp naphthalene-moiety absorption features are found in the spectrum of A3N. Our explanation is that energy transfer from the naphthalene chromophore to the anthracene chromophore in A3N is much faster than that of A1N. Fast EET results in homogeneous broadening such that these features are very broad and weak. In the spectrum, they are hidden beneath the anthracene moiety background and cannot be observed.

Based on this idea, we can make a very rough estimate of the EET rate for A3N. In the spectrum of A1N (Figure 4c), the ratio of peak intensity to baseline noise is about 20:1. If all the

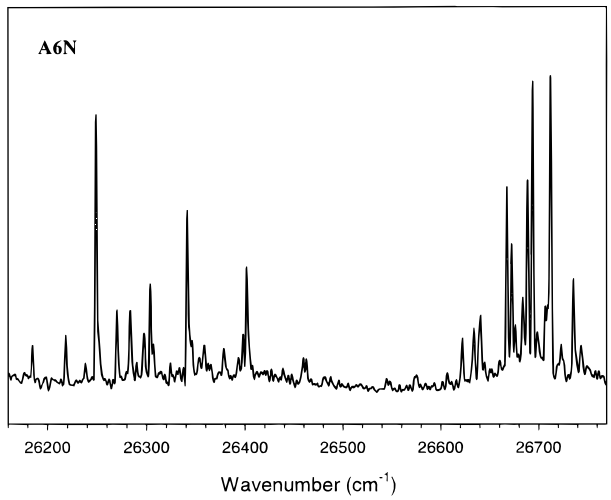

Figure 8. Total fluorescence excitation spectrum of A6N in range of the anthracene moiety S_0-S_1 transition.

peaks are broadened more than 20 times, they will be hidden inside the noise. Therefore, the EET rate is greater than 1.5×10^{13} s^{-1}.

3.4 Anthracene−(CH2)$_6$−Naphthalene (A6N). Figure 8 is the total fluorescence excitation spectrum of A6N in the anthracene moiety S_0-S_1 origin. The 0−0 transition is at 26 249 cm^{-1}. It is red-shifted 1446 cm^{-1} from the origin of anthracene, 684 cm^{-1} from the origin of 9MA, 542 cm^{-1} from the origin of A1N, and 448 cm^{-1} from the origin of A3N. Such large red shifts are the signs of a strong inter-chromophore interaction and solvent effect in A6N. A few bands appearing to the red of the 0−0 transition are assigned as hot bands. There are several transitions near the origin with excess energies of 21, 35, 48, and 55 cm^{-1}. These peaks can be assigned as either the torsional modes of the $-(CH_2)_6-$ chain or large amplitude interchromophore motion. Two peaks of 93 cm^{-1} and 152 cm^{-1} excess energy have compatible intensity to the 26249 cm^{-1} peak. They might be assigned as the vibronic modes built on top of the 26249 cm^{-1} peak or the transition origins of two other conformers of A6N. The group of peaks with excess energy of 370 cm^{-1} to 500 cm^{-1} is built on top of the 12_0^1 anthracene transition.

The dispersed fluorescence spectrum of A6N is a typical anthracene-type emission spectrum looking like that of anthracene and other anthracene derivatives.

The total fluorescence excitation spectrum of A6N was also scanned from 30 550 to 33 150 cm^{-1}, the naphthalene moiety range. As with A3N, the spectrum is basically a continuum background and does not contain any sharp peaks. It can be concluded that energy transfer from the naphthalene chromophore to the anthracene chromophore in A6N is also much faster than that in A1N, and the same estimation procedure of the EET rate used for A3N can be applied to A6N.

4. Discussion

The experiments described in the last section have shown that the A*n*N bichromophoric system is not an unusual system in terms of the Intra-EET efficiency. The EET rate in A1N is 6.7×10^{11} s^{-1} rather than 3×10^6 s^{-1} or 5×10^6 s^{-1} as reported in a previous paper,[11] and the EET rates in A3N and A6N are at least 2 orders of magnitude faster than that of A1N. The biggest difference between the A1N fluorescence excitation spectrum in the naphthalene moiety range reported in this paper and that which was previously published[11] is that the latter contain many long-lifetime peaks. These peaks may be due to dinaphthalene impurities.

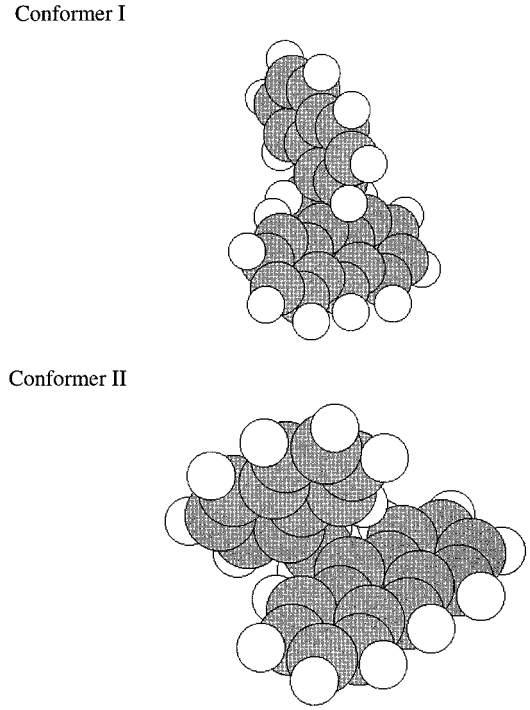

Figure 9. Calculated A1N geometry.

To help the interpretation of the experimental results, we performed molecular mechanics calculations to estimate the geometry of A*n*N molecules in their ground states. Our geometry optimizations were carried out using MM+ (an improved MM2[26] force field in the HyperChem[27] package running on a PC) or MMFF (in the Spartan[28] package running on Unix workstation) force fields. When doing geometry optimizations using these packages, the result is usually a local minimum on the potential energy surface rather than a global minimum. The local minimum found by the program depends on the initial guess for the geometry, and therefore, a search for the global minimum requires many calculations, each using a different starting geometry.

Our starting geometries for the anthracene and naphthalene moieties were generated from standard bond lengths and angles and were not varied. We generated different starting geometries by varying the conformation of bridge linking the two moieties. For A1N, we varied the twisting angle of each aromatic plane with respect to the bond between the aromatic and the bridge carbon. We varied the twist angle of both the anthracene and the naphthalene planes in increments of 10 degrees. For A3N and A6N, we used as initial geometries all possible conformations of the bridge chain where the carbon−carbon bonds were either gauche or trans. In the case of A3N and A6N, we did not vary the twist angle of the aromatic planes. It should be emphasized that the variation described here was of the initial geometry. From each initial geometry, the program then found an optimized geometry.

Two low-energy conformers of A1N identified by these calculations are shown in Figure 9. Their calculated energies are close enough that, within the precision of the calculation, either could be the lowest-energy conformer.

For A3N and A6N, the polymethylene chain is more flexible and allows many possible conformers. All calculated geometries fall into two categories. One contains conformations in which the two chromophores are face-to-face, forming a sandwiched

configuration. The other category includes conformations in which the $-(CH_2)_n-$ chain is stretched out and the two chromophores are separated. We calculate that in a face-to-face binary complex of anthracene and naphthalene, the binding energy is around 8 kcal/mol. However, in the covalently bound bichromophore, some energy must be expended to bring the polymethylene chain into a configuration where the two aromatics can be face-to-face. One gauche conformation in the polymethylene chain is around 1−1.5 kcal/mol[29] less stable than one trans conformation. Thus, a face-to-face configuration of the A*n*N molecule requires more than 8 gauche conformations in the chain, and it is less stable than the stretched-out conformer. If a face-to-face configuration requires less than 5 gauche conformations in the chain, it is probably more stable than the stretched-out conformer. In addition to the thermodynamic stability of the two types of conformers, the kinetics of relaxation in the jet must be considered. If the energetics allow for a mixture of conformers at the temperature of the nozzle, there may be little or no relaxation of that distribution in the expanding jet, and the observed distribution is likely to be characteristic of the nozzle temperature rather than the downstream temperature of the jet. In this case, the entropic contribution to the free energy at the nozzle temperature, a quantity not considered in the molecular mechanics calculations, may be significant.

The lowest-energy conformation calculated for A3N is a face-to-face sandwich-type conformer with two gauche conformations in the bridge chain. The distance between the two chromophores is only 3.3 Å, and there is a large overlap of the wave functions. Fast EET is expected for this conformer since both the Förster and Dexter mechanisms can make significant contributions to EET. In a typical stretched-out-type conformer, the separation of the two chromophores is about 8.3 Å. We calculate that the face-to-face conformer is about 2500 cm^{-1} more stable than the stretched-out conformer. The situation for A6N is similar to A3N. The face-to-face conformer has three gauche conformations, and its interchromophore distance is 4.2 Å.

The S_1 state of naphthalene is positioned about 5000 cm^{-1} above the S_1 state of anthracene (see Figure 2). EET in A*n*N can be treated within the framework of radiationless transition theory.[30,31] In the present case, when D and A are different and a sizable energy gap exists between the electronically excited states of these two chromophores, the density of vibronic states in A* (anthracene) is high near the zero-point level of the D* state (naphthalene). Therefore, the EET process in A*n*N falls in the statistical limit,[30,31] and its rate can be described by a Golden-Rule-like expression, which under the Born−Oppenheimer approximation becomes

$$k_{EET} = \frac{2\pi}{\hbar}\mathrm{FCWD}|\langle\theta_{D^*A}|H'|\theta_{DA^*}\rangle|^2 \qquad (2)$$

where H′ is the interaction Hamiltonian, θ_{D^*A} and θ_{DA^*} are the electronic parts of the wave functions, and FCWD is the Franck−Condon weighted density of states.

Förster's theory[7] deals with the Coulomb contribution to H′, which is approximated by dipole−dipole interaction, for which the EET rate constant is given by

$$k_{EET} = \frac{2\pi}{\hbar}\mathrm{FCWD}|\frac{\mu_D\mu_A\kappa}{R^3}|^2 \qquad (3)$$

where μ_D and μ_A are the magnitude of the electronic transition dipole moments of D and A, respectively. R is the distance between the two dipole moments, and κ is the orientation term given by

$$\kappa = \cos\alpha_{DA} - 3\cos\alpha_{DR}\cos\alpha_{RA} \qquad (4)$$

where, α_{DA}, α_{DR} and α_{RA} are the angles between the vectors μ_D and μ_A, μ_D and **R**, and **R** and μ_A, respectively.

TABLE 4: Comparison of the Förster Contributions to EET in the Calculated A1N, A3N, and A6N Conformations

conformer	A1N (I)	A1N (II)	A3N (I)	A6N (I)
α_{DA} (^{0})	25	50	75	75
α_{DR} (^{0})	45	90	75	90
α_{RA} (^{0})	20	45	90	60
κ	−1.09	0.642	0.259	0.259
R (Å)	5.7	4.8	3.3	4.2
κ^2/R^6 (Å^{-6})	3.5×10^{-5}	3.4×10^{-5}	5.2×10^{-5}	1.2×10^{-5}

The transition dipole of the anthracene S_0-S_1 transition is short-axis polarized,[32] whereas the transition dipole of the naphthalene S_0-S_1 transition is long-axis polarized. The transition dipoles in 1MN and 9MA have similar polarizations. The orientation factor, κ, and R in eq 3, derived from the calculated geometries of A*n*N, are shown in Table 4. The values for κ shown in Table 4 are based on the assumption that the directions of the transition dipoles do not change in the bichromophore.

The contributions from the term κ^2/R^6 in the Förster mechanism are similar in A1N, A3N, and A6N. Therefore, the Förster mechanism does not explain the 2 orders of magnitude difference between the EET rate in A3N and A6N as compared to A1N. Moreover, chromophores are sufficiently close that the dipole−dipole approximation is unlikely to be valid.

The longer chains in A3N and A6N introduce extra stretching, bending, and torsional modes that are not available in A1N, leading to a greatly increased density of vibronic states. Even though many such chain modes may not have good Franck−Condon factors, the FCWD in eq 4 will be larger for A3N and A6N than for A1N. Probably more important, since both A3N and A6N form a face-to-face conformation in the jet, the exchange mechanism for EET must play a larger role for them than for A1N. For the exchange mechanism, it has been shown that the orientation of the two chromophores is important in addition to the traditional exponential distance dependence in the Dexter model. This is different from the solution situation where A1N also exhibits the same, ultrafast Intra-EET due to dipole−dipole intearctions.[6,33]

5. Summary

The intramolecular electronic energy transfer (EET) process for a series of molecules 1-naphthyl−$(CH_2)_n$−9-anthryl (n = 1, 3, and 6) was investigated in a supersonic jet. For n = 1 (A1N), S_0-S_1 fluorescence excitation spectra of both anthracene and naphthalene moieties were observed. When the naphthalene moiety is excited, the emission contains only anthracene-like fluorescence, showing that the EET rate from the naphthalene moiety to the anthracene moiety is much faster than the naphthalene fluorescence lifetime. From the measurements of homogeneous broadening, the EET rate is estimated to be 6.7×10^{11} s^{-1}. For n = 3 (A3N) and n = 6 (A6N), only fluorescence excitation spectra of the anthracene moiety are observed. Sharp naphthalene moiety transitions are not observed and are assumed to be buried under the anthracene moiety absorption continuum. This implies that the EET rate in A3N and A6N is much faster than in A1N. The faster EET in A3N and A6N is explained by the larger FCWD and by the

contribution of an exchange mechanism allowed by the formation of face-to-face inter-chromophore configurations.

Acknowledgment. We are grateful to Dr. Irina Fedatov for preparation of the bichromophoric molecules. This work was supported in part by the Technion V.P.R. Fund for the Promotion of Research at the Technion and by Grant number 96-00171 from the US−Israel Binational Science Foundation. The work at Chicago was supported by the National Science Foundation under Grant CHE-9319958.

References and Notes

(1) Speiser, S. *Chem. Rev.* **1996**, *96*, 1953.
(2) Ebata, T.; Suzuki, Y.; Mikami, N.; Miyashi, T.; Ito, M. *Chem. Phys. Lett.* **1984**, *110*, 597.
(3) Chattoraj, M.; Bal, B.; Closs, G. L.; Levy, D. H. *J. Phys. Chem.* **1991**, *95*, 9666.
(4) Chattoraj, M.; Bal, B.; Shi, Y.; Closs, G. L.; Levy, D. H. *J. Phys. Chem.* **1993**, *97*, 13046.
(5) Chattoraj, M.; Chung, D. D.; Bal, B.; Closs, G. L.; Levy, D. H. *J. Phys. Chem.* **1994**, *98*, 3361.
(6) Schnepp, O.; Levy, M. *J. Am. Chem. Soc.* **1962**, *84*, 172.
(7) Förster, Th. *Discuss. Faraday Soc.* **1959**, *27*, 7. Förster, Th. *Modern Quantum Chemistry*; Sinanoglu, O., Ed.; Academic Press: New York, 1968; Vol. 3, p 93.
(8) Dexter, D. L. *J. Chem. Phys.* **1953**, *21*, 836.
(9) Bigman, J.; Karni, Y.; Speiser, S. *Chem. Phys.* **1993**, *177*, 601.
(10) Liao, D. W.; Cheng, W. D.; Bigman, J.; Karni, Y.; Speiser, S.; Lin, S. H. *J. Chin. Chem. Soc.* **1995**, *42*, 177.
(11) Rosenblum, G.; Grosswasser, D.; Schael, F.; Rubin, M. B.; Speiser, S. *Chem. Phys. Lett.* **1996**, *263*, 441.
(12) Rosenblum, G.; Speiser, S. *J. Photochem. Photobiol., A* **1998**, *112*, 117.
(13) Rona, P.; Feldman, U. *J. Chem. Soc.* **1958**, 1737.
(14) Sharfin, W.; Johnson, K. E.; Wharton, L.; Levy, D. H. *J. Chem. Phys.* **1985**, *71*, 4990.
(15) Lambert, W. R.; Felker, P. M.; Syage, J. A.; Zewail, A. H. *J. Chem. Phys.* **1984**, *81*, 2195.
(16) Fischer, S. F.; Lim, E. C. *Chem. Phys. Lett.* **1974**, *26*, 312.
(17) Beck, S. M.; Powers, D. E.; Hopkins, J. B.; Smalley, R. E. *J. Chem. Phys.* **1980**, *73*, 2019.
(18) Stockburger, M.; Gattermann, H.; Klusmann, W. *J. Chem. Phys.* **1975**, *63*, 4519.
(19) Van Dantzig, N. A. Ph.D. Thesis, University of Chicago, 1994; Chapter 3.
(20) Syage, J. A.; Felker, P. M.; Zewail, A. H. *J. Chem. Phys.* **1984**, *81*, 2233.
(21) Warren, J. A.; Hayes, J. M.; Small, G. J. *J. Chem. Phys.* **1984**, *80*, 1786. The signal-to-noise ratio in Figure 4a (the naphthalene chromophore) is lower than that of Figure 3a (the anthracene chromophore). This is because the intensity of the 9MA spectrum ($\epsilon_{max} = 8500$ cm^2 mol^{-1}) is considerably higher than that of the 1MN spectrum ($\epsilon_{max} = 340$ cm^2 mol^{-1}). See Birks, J. B. *Photophysics of Aromatic Molecules*; Wiley-Interscience: London, 1970; p 70.
(22) Jacobson, B. A.; Guest, J. A.; Novak, F. A.; Rice, S. A. *J. Chem. Phys.* **1987**, *87*, 269.
(23) Behlen, F. M.; Rice, S. A. *J. Chem. Phys.* **1981**, *75*, 5672.
(24) Lambert, W. R.; Felker, P. M.; Zewail, A. H. *J. Chem. Phys.* **1981**, *75*, 5958.
(25) Amirav, A.; Sonnenschein, M.; Jortner, J. *J. Phys. Chem.* **1984**, *88*, 5593.
(26) Allinger, N. L. *J. Am. Chem. Soc*. **1977**, *99*, 8127.
(27) *HyperChem for Windows*, reference manual, Autodesk, Inc., 1993.
(28) Hehre, W. J.; Yu, J.; Klunzinger, P. E. *A Guide to Molecular Mechanics and Molecular Orbital Calculations in Spartan*; Wave functions Inc., 1997.
(29) Eliel, E. L. *Stereochemistry of Carbon Compounds*; MacGraw-Hill: New York, 1962.
(30) Bixon, M.; Jortner, J. *J. Chem. Phys.* **1968**, *48*, 715.
(31) Bixon, M.; Jortner, J. *J. Chem. Phys.* **1969**, *50*, 3248, 4061.
(32) Platt, J. R. *J. Chem. Phys.* **1949**, *17*(5), 484.
(33) Schael, F.; Rubin, M. B.; Speiser, S. *J. Photochem. Photobiol., A* **1998**, *115*, 99.